NANO LETTERS

Letter

pubs.acs.org/NanoLett

Quantum Confined Electron–Phonon Interaction in Silicon Nanocrystals

D. M. Sagar,*[,†] Joanna M. Atkin,[‡] Peter K. B. Palomaki,[†] Nathan R. Neale,[†] Jeffrey L. Blackburn,[†] Justin C. Johnson,[†] Arthur J. Nozik,[†,§] Markus B. Raschke,[‡] and Matthew C. Beard*[,†]

[†]Chemistry & Nanoscience Center, National Renewable Energy Laboratory, Golden, Colorado 80401, United States

[‡]Department of Physics, Department of Chemistry, and JILA, University of Colorado, Boulder Colorado 80309, United States

[§]Department of Chemistry and Biochemistry, University of Colorado, Boulder Colorado 80309, United States

Supporting Information

ABSTRACT: We study the micro-Raman spectra of colloidal silicon nanocrystals as a function of size, excitation wavelength, and excitation intensity. We find that the longitudinal optical (LO) phonon spectrum is asymmetrically broadened toward the low energy side and exhibits a dip or antiresonance on the high-energy side, both characteristics of a Fano line shape. The broadening depends on both nanocrystal size and Raman excitation wavelength. We propose that the Fano line shape results from interference of the optical phonon response with a continuum of electronic states that become populated by intraband photoexcitation of carriers. The asymmetry exhibits progressive enhancement with decreasing particle size and with increasing excitation energy for a given particle size. We compare our observations with those reported for p- and n-doped bulk Si, where Fano interference has also been observed, but we find opposite wavelength dependence of the asymmetry for the bulk and nanocrystalline Si. Our results have important implications for potentially controlling carrier energy relaxation channels in strongly confined Si nanocrystals.

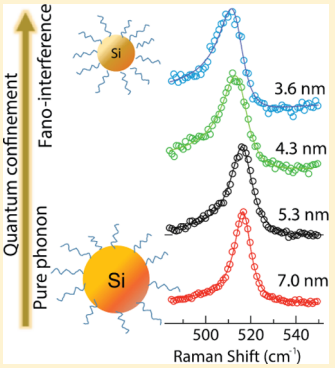

KEYWORDS: *Electron–phonon coupling, silicon nanocrystals, Raman spectroscopy, carrier energy relaxation, Fano-interference*

We report an investigation of the electron–phonon (e–ph) interactions in colloidal quasi-spherical Si nanocrystals (NCs), also referred to as quantum dots (QDs), using micro-Raman scattering. Electron–phonon coupling mediates carrier energy relaxation in bulk semiconductors and is modified in semiconductor NCs.[1−3] Thus, understanding and potentially controlling e–ph interactions is a central issue in semiconductor NC research and can allow for control of carrier dynamics and energy relaxation. While a number of prior Raman spectroscopy studies have explored e–ph interactions in Si NCs, there is still a lack of agreement on the origin of the observed asymmetry in the one-phonon Raman spectrum of the LO phonon mode. Previous studies have attributed this asymmetry to several physical phenomena, including phonon confinement,[4,5] Fano interference,[6] or a combination of Fano and phonon confinement.[7] Furthermore, the influence of *extrinsic* factors, such as surface charges, on e–ph coupling remains unclear.

In this work, we extend previous studies by varying the excitation wavelength, excitation intensity, and average particle size to gain a deeper fundamental understanding of the origin of LO phonon line shape asymmetry in Si NCs. We find that the Raman line shape for the LO mode in Si NCs is best described by the Breit–Wigner–Fano (BWF) model,[8] wherein a continuum of electronic states gives rise to a quantum interference with the one-phonon response resulting in an asymmetric LO phonon spectrum. Within this BWF model, the so-called Fano factor describes the strength of the interference and is associated with the degree of asymmetry. We find an increase in asymmetry (increasing Fano factor) with both increasing excitation energy, as well as decreasing average particle diameter for a given excitation energy. We compare our results to that reported for doped bulk Si where a Fano line shape is also observed, but we find a different dependence of the asymmetry on the excitation wavelength, suggesting that the e–ph interaction can be modified in colloidal Si NCs. Our results provide fundamental insights into critical parameters that influence the e–ph coupling in Si NCs and help to clarify discrepancies in previous studies. Additionally, the size-dependent e–ph interaction in Si suggests potential routes for controlling energy relaxation channels within nanostructures based on colloidal NCs.

Colloidal Si NCs were synthesized from a nonthermal plasma reactor as described previously,[9−11] with details in the Supporting Information (SI). After synthesis, the hydrogen-terminated NCs undergo a thermally initiated hydrosilylation reaction to attach dodecyl ligands. The dodecyl ligands serve at least three purposes: (1) they allow the NCs to be dispersed as colloids in nonpolar solvents, such as hexane; (2) they passivate surface defects resulting in improved emission; and (3) they

Received: September 24, 2014
Revised: January 9, 2015
Published: January 27, 2015

DOI: 10.1021/nl503671n
Nano Lett. 2015, 15, 1511−1516

reduce the rate of oxidation.[9] We studied four samples that are characterized by peak photoluminescence (PL) energies of 1.24, 1.29, 1.44, and 1.55 eV. Using a sizing curve[11] to relate the peak PL energy to NC diameter, our samples correspond to average diameters of 7.0, 5.3, 4.3, and 3.6 nm, respectively. However, we refer to the samples by their peak PL energy, as this parameter is a better sample indicator due to uncertainties in determining NC physical size.

Raman measurements were carried out on NC films deposited from hexane colloids on a sapphire substrate and subsequently sealed in an air-free sample holder during measurements to minimize degradation (additional details in the SI). The Raman spectra at three different excitation wavelengths (633, 532, and 488 nm) were collected using two different home-built Raman systems, in epi-illumination mode. In the first micro-Raman system, the 532 and 633 nm excitation beams were focused with an extra-long working distance objective (Olympus, 0.5 numerical aperture), with a total power at the sample of 1−6 mW (1.8−12 kW/cm^2), and focus size of ∼4 μm. The scattered light was spectrally filtered with a long-pass Raman filter, with 140 cm^{-1} cutoff. It was then detected with a spectrometer with 1200 g/mm grating (Princeton Instruments) and liquid nitrogen cooled CCD (Acton Research). For the second system, the 532 nm CW excitation beam was focused onto the sample with a spot size of ∼200 μm, with powers in the range of 5−120 mW (∼16−290 W/cm^2). With 488 nm excitation, the spot size was ∼200 μm, with typical laser power in the range of 5−30 mW (∼4−20 W/cm^2). The excitation energy in each case is above band-edge electronic excitation for the Si NCs as estimated from the PL spectrum.

Figure 1a shows representative TEM images taken from two of the Si NC samples (the smallest and largest) with peak PL

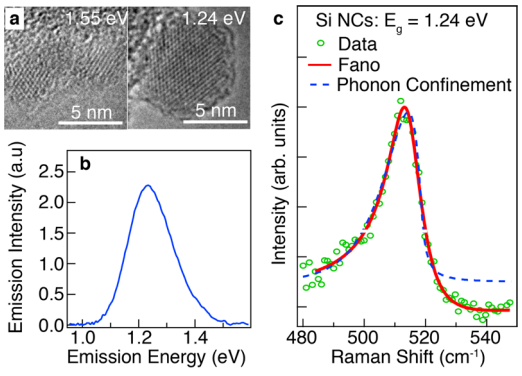

Figure 1. (a) Representative TEM images of d = 3.6 nm (PL peak energy 1.55 eV) and d 7.0 nm (PL peak 1.24) Si NCs. (b) A typical PL spectrum of the d = 7.0 nm sample. (c) Raman spectrum of the LO mode for λ_{Exc} = 532 nm (green circles) for d = 7.0 nm. The data are modeled using both the Fano model (red trace) and the phonon confinement model (blue dashed trace).

energies of 1.55 and 1.24 eV. A wider field image of the 1.24 eV sample is shown in Figure S1, in addition to a size histogram used to determine the log-normal size-dispersion with <20%[11] variation in diameter. The TEM images show that the NCs have highly crystalline cores with an outer layer that has some degree of disorder (amorphous character) and an amorphous organic ligand shell. The NCs are roughly spherical but vary in shape (see Figure S1). Figure 1b shows the PL spectrum for the 7.0 nm sample with peak PL energy of 1.24 eV. The width of the PL is dictated by the size distribution.[12]

Figure 1c shows the Raman spectrum of the LO phonon mode of Si NCs with peak PL energy of 1.24 eV, for 532 nm excitation at ∼4 mW. The LO-phonon mode presented here has been decomposed from the raw data. The raw spectra (see Figures S3−S5) show vibrational features associated with surface ligand vibrations and vibrational modes of amorphous-Si (a-Si). We verified the positions of the ligand vibrations by independent Raman measurements of the ligands without NCs (data not shown). The features we associate with a-Si correspond with those in literature reports.[13] In our deconvolution procedure, we fit all of the low-frequency modes with Lorentzian lineshapes, where the Lorentzian peak energies are fixed at the various phonon modes of a-Si[14] and the measured ligand modes, and then subtract those peaks from the raw data (Figures S3−S5). In each data set, the relative contribution of the a-Si and ligand vibrations varies depending on the laser excitation wavelength and power level, but the peak positions and line widths did not. Such deconvolution of interfering fluorescence background and/or background peaks in Raman spectroscopy is a commonly adopted procedure.[15,16] We note that our subtraction procedure does not modify the c-Si phonon line shape, since essential features on the blue edge of the peak, which do not have interfering modes, are unchanged after subtraction. Figure 1c demonstrates a clear asymmetry of the LO phonon line shape for our largest diameter (∼7.0 nm) Si NCs, with PL energy of 1.24 eV. We observe an asymmetric LO phonon spectrum for all the Si NCs studied (*vide infra*).

Asymmetric lineshapes and the observation of a frequency redshift with respect to bulk Si for the LO phonon in Si nanostructures have been reported in the literature[4,7,12,6,17] and are the source of much debate. As such, it is useful to briefly discuss the physical mechanisms and resulting models that may be used to reproduce the asymmetric LO phonon line shape. In microcrystalline Si, the observed asymmetry has been explained by the phonon-confinement model of Richter, Wang, and Ley (RWL)[4] (SI). The RWL model is based on the relaxation of the q-vector selection rule in dimensionally confined systems, giving rise to the activation of modes away from the zone center ($q \neq 0$) in addition to the $q = 0$ phonons at the center of the Brillouin zone. The continuum of modes with $q \neq 0$ adds up to produce the asymmetry in the phonon spectrum. In solid systems, such symmetry breaking modes typically arise from disorder.[18] In the RWL model the observed frequency redshift (with respect to the bulk LO energy) for smaller NCs is governed by the phonon dispersion. In contrast, some researchers have ascribed the asymmetry on the low frequency side to interface states associated with a disordered surface[13] where bond lengths and angles can vary from the crystalline core. We find that neither of these explanations can adequately describe all features of our data, as discussed in more detail below.

An asymmetric LO phonon mode was also observed in bulk silicon under both n- and p-doping conditions.[19,20] In this case the asymmetry was interpreted as arising due to the Fano-interference of the discrete LO phonon mode with a continuum of either electron (n-type) or hole (p-type) excitations. Interference of the electronic continuum with the discrete LO phonon produces an asymmetry toward the low frequency side accompanied by a frequency redshift, while interference of the hole continuum produces a high frequency asymmetry with

DOI: 10.1021/nl503671n
Nano Lett. 2015, 15, 1511−1516

a frequency blueshift.[6] In that work, Gupta et al. suggested that laser-induced Fano coupling in Si nanowires gives rise to a power-dependent LO line shape and energy. The LO lineshape was found to be symmetric at very low excitation densities, but increasing laser power induced a redshift in frequency and increased asymmetry toward the low energy side of the main LO mode.[6] The evolution of the Fano profile with excitation laser power was interpreted as a strong signature of the LO mode coupling to the photoexcited electronic continuum. Similar intensity-dependent Fano lineshapes were reported by Kumar et al. for laser-etched silicon nanostructures.[7]

In Figure 1c we compare the ability of both the phonon-confinement model (dashed blue line) and the Fano model (solid red line) to describe our data. Although the phonon confinement model (full equation in SI) reproduces the low-frequency asymmetry, it cannot account for the consistently observed *dip* or *antiresonance* toward the higher frequency side of the LO mode.[12,17] The Raman intensity, $I(\omega)$, for the Fano model is given by

$$I(\omega) = A\frac{(q+\varepsilon)^2}{q+\varepsilon^2} \quad (1)$$

where $\varepsilon = (\omega - \omega_0)/\Gamma$, ω_0 is the renormalized or "*dressed*" phonon frequency in the presence of the Fano coupling, $|1/q|$ is the ratio of the resonant to nonresonant contribution (sometimes known as the "Fano factor" or asymmetry factor), and Γ is the line width (related to the phonon lifetime). From a linear least-squares fitting procedure we obtain $|1/q| = 0.16$, $\Gamma = 6.4$ cm^{-1}, and $\omega_{LO} = 515.6$ cm^{-1}, i.e., a shift of almost 5 cm^{-1} compared to bulk Si with $\omega_{LO} = 520$ cm^{-1}.

Raman spectra of the LO phonon mode for Si NCs of various sizes are shown in Figure 2a. Each spectrum in Figure 2a (open circles) is fit with a Fano line shape (solid lines, eq 1), and the resulting parameters obtained from each fit are displayed in Figure 2b–d. A redshift in the peak frequency (panel d) and increases in the line width (panel c) and the asymmetry factor (panel b) are found with decreasing average particle size. The asymmetry factor increases to as high as ~0.32 for the smallest NC size measured, with a peak shift of 5 cm^{-1}. For larger diameter NCs, the line shape evolves to more closely resemble that found in undoped bulk Si.

Several other groups have reported a frequency redshift of several cm^{-1} (with respect to bulk Si) that depends on the NC diameter.[4,6,7,12] For example, Hessel et al. reported NC size-dependent frequency shifts of the asymmetric LO mode,[12] similar to what is observed here. They compared their data to both a phonon confinement model and a bond polarization model[5] and found that both models failed to reproduce the large redshift in smaller NCs.

To further elucidate the origin of the asymmetry in the LO phonon mode in the strong quantum confinement limit in Si NCs, we performed Raman scattering experiments for three different wavelengths. The data for 5.3 nm Si NCs with E_{PL} = 1.29 eV, excited at 488 nm, 532 nm, and 633 nm, respectively are shown in Figure 3a with the corresponding Fano line shape fits (solid lines). Also shown in Figure 3a is the spectrum for intrinsic c-Si, with excitation at 532 nm; the c-Si sample is best fit with a Lorentzian line shape (solid line) with an energy and width that are invariant with excitation wavelength. For the 5.3 nm Si NCs, the asymmetry factor (Figure 3b) and line width (Figure 3c) both increase as a function of increasing excitation energy.

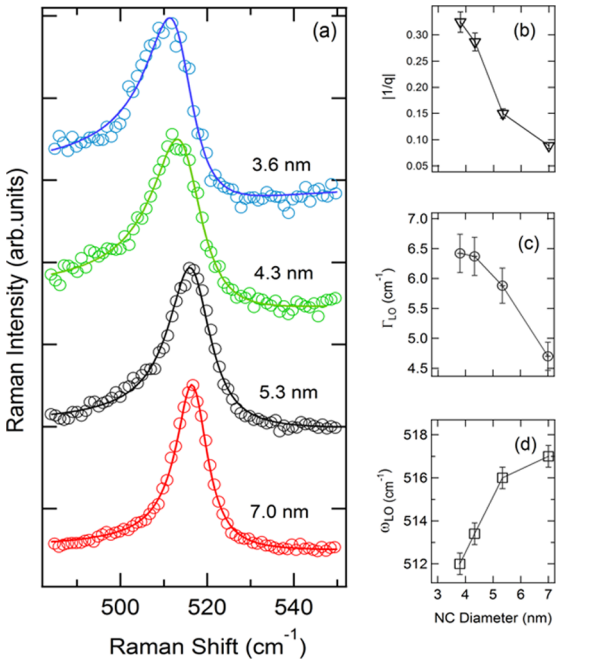

Figure 2. (a) Raman spectra of the four samples studied with excitation at 532 nm, 4 mW. Data are the symbols, and the solid lines are best-fit Fano model. The traces are vertically offset for clarity. (b–d) Best-fit parameters of the model as a function of NC diameter; (b) is the Fano factor $|1/q|$, (c) line width Γ_{LO}, and (d) the peak frequency ω_{LO}. The solid lines in b, c, and d are guides to the eye. The excitation intensities were kept the same for all the samples.

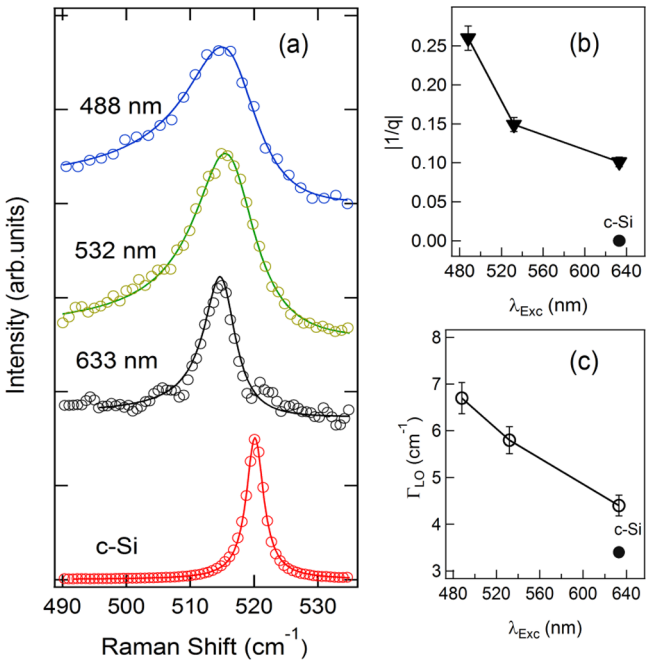

Figure 3. (a) Excitation wavelength-dependent Raman spectra of the LO mode for the 5.3 nm (E_{PL} = 1.29 eV) sample with the Raman spectrum for bulk intrinsic c-Si shown for comparison and collected on the same setup as the NC samples (data are offset vertically for clarity). (b) and (c) show the asymmetry factor and line width as a function of excitation wavelength.

A particularly striking feature of the data in Figure 3 is the observation of a near-Lorentzian line shape when the Si NCs are excited at 633 nm, which is contrary to the predictions of

DOI: 10.1021/nl503671n
Nano Lett. 2015, 15, 1511–1516

the phonon confinement model[4] (see Discussion below). The near-Lorentzian line shape is similar to that of bulk Si, although the frequency is red-shifted with respect to bulk Si. The evolution of line shape from near-Lorentzian to Fano as the incident energy is increased is in striking contrast with p-type bulk silicon, where the opposite trend is observed.[21] Further, the line width is independent of excitation wavelength in bulk silicon. The enhancements in the asymmetry factor and line width at higher excitation energies indicate stronger Fano coupling and a reduced LO mode lifetime, respectively, due to stronger e−ph coupling. Experiments exciting the QDs with a subresonant wavelength of 1064 nm (data not shown) were found to have a signal too weak for accurate analysis.

In Figure 4 we display the excitation intensity-dependence of the LO mode for d = 3.6 nm NCs (E_{PL} = 1.55 eV). As the intensity is increased, the LO phonon mode redshifts, as shown in the inset. Even for the lowest power measured of 5 mW (~16 W/cm^2), the line shape remains asymmetric. The frequency redshift tends to saturate at higher intensities. The line width and asymmetry factor (not shown) tend to increase with increasing laser intensity, although the trend is not as smooth as observed for the frequency shift. While in the low intensity range, 16−290 W/cm^2, a systematic intensity-dependent redshift is observed (Figure 4), in the high intensity regime (≳10 kW/cm^2) we do not observe any change in the LO phonon mode (Figure S8, SI). The frequency, line width, and asymmetry factor at higher intensities do not change, suggesting saturation of the electronic continuum.

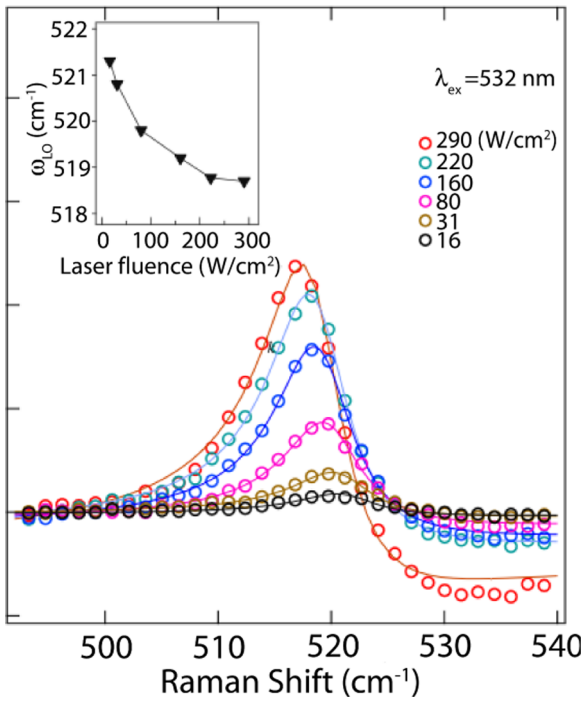

Figure 4. Line shape of the LO mode for 3.6 nm (E_{PL} = 1.55 eV) Si QDs at 532 nm excitation. The background has been subtracted as discussed in the Supporting Information so that the intensities at 495 cm^{-1} overlap. The inset shows the frequency shift versus incident laser intensity.

We interpret the combination of results above in light of the Breit−Wigner−Fano model rather than a phonon confinement model for the following reasons. (1) The asymmetric line shape observed in all the data cannot be modeled using the phonon confinement model, as demonstrated by the fits shown in Figure 1. Particularly, the observed "antiresonance" dip toward the higher energy side is not reproduced in the phonon confinement model. (2) The dependence of the asymmetry factor on excitation energy does not support the phonon confinement model and suggests the involvement of photo-excited carriers. For instance, at 633 nm excitation a near-Lorentzian line shape is observed for QD diameter of 5.3 nm. For phonon confinement, the asymmetry should be invariant with excitation energy. (3) The asymmetry factor tends to increase (see Figure 4), suggestive of coupling of the LO mode with photoexcited carriers. (4) For the smallest particle size measured, 3.6 nm, the line shape is distinctly Fano-like and cannot readily be described by other line shape models. For smaller particles the phonon confinement is expected to be stronger and would lead to a higher degree of asymmetry, similar to what is observed here.

Additional support for the interpretation of our data within the Breit-Wigner-Fano model is provided by a comparison to doped bulk Si. Fano interference of the LO mode with the electronic and hole continuum has been observed in heavily doped bulk silicon and explained by Contreras et al. by considering interference with spin−orbit bands with a relatively flat density of states.[20] In a single-particle phonon model, the one-phonon line is well described by a pure Lorentzian, as seen in intrinsic c-Si (Figure 3). Upon interference with an electronic continuum, the scattering line shape is modified to an asymmetric Fano line shape, with an asymmetry proportional to the degree of e−ph interaction. Due to the interference effect, the resulting feature cannot be simply described as a single particle phonon, rather a composite quasiparticle or a collective excitation also called *interferon*.[22] Regardless of doping density, LO phonons in doped Si can always find a continuum of states within their energy range to couple. In contrast, such energetics are not favored in germanium, where the LO phonon energy is much smaller (37 meV) than the spin−orbit splitting (300 meV).

The interaction strength between the LO phonon mode and the electronic continuum is quantified by the parameter $|1/q|$. The coupling strength $|1/q|$ is proportional to $|R_e/R_p|$, where R_e is the probability of scattering of incident radiation by the electronic continuum and R_p is the probability of scattering due to the discrete LO phonon. The interference causes resonance and antiresonance in the one-phonon Raman spectrum leading to the asymmetric Fano line shape. For Fano interference in p-doped bulk silicon, the source of electronic continuum was identified as arising from intervalence band transitions due to spin orbit splitting.[21] The spin−orbit energy in bulk Si is ~44 meV, while ω_{LO} = 65 meV. Therefore, regardless of carrier concentration due to doping, the LO mode is always in resonance with a continuum of electronic states. For bulk Si, the LO mode line width is invariant with excitation wavelength and the asymmetry $|1/q|$ decreases with decreasing excitation wavelength. These observations were explained by the assumptions of nonvarying density of continuum states in the valence band of bulk silicon.[21] In the case of Si NCs reported here, a strikingly different behavior is observed. From the excitation wavelength dependent data presented in Figure 3, the asymmetry and line width both increase with decreasing excitation wavelength. These observations suggest that, unlike in bulk Si, the interfering electronic continuum DOS shifts in energy with nanoparticle size and excitation wavelength.

DOI: 10.1021/nl503671n
Nano Lett. 2015, 15, 1511−1516

To explain the difference in wavelength-dependent LO phonon response between Si NCs and bulk Si, two possible scenarios are considered that can give rise to the observed Fano interference. In the first case, the LO phonon interferes with an electronic continuum arising from photoexcited electrons above the bandgap. Recent DFT calculations suggest that quantum confinement modifies the continuous density of states producing mini-gaps and narrow band-like levels (see Figure 5).[23] The Raman excitations used here are resonant, since the

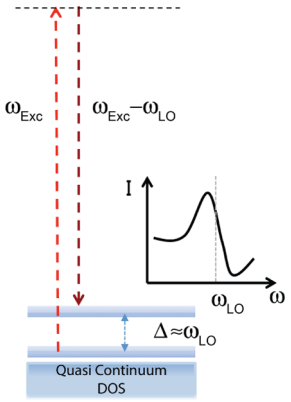

Figure 5. A qualitative picture describing the proposed model that can explain the observed size-dependent Fano interference. Quantum confinement leads to a density of states that is quasi-continuous with mini-gaps whose energy depend on size and can approach the LO-phonon energy providing an electronic continuum for the Fano interference.

excitation energy is greater than the PL energy. Upon interband photoexcitation of electron−hole pairs, the resultant excitonic wave function is asymmetric due to the dissimilarity in the band structures of electrons and holes. In other words, the lighter electron can decouple from the hole and can undergo intraband relaxation via emission of optical phonons. The rate of phonon emission depends upon the intraband quantum level spacing (Δ in Figure 5), which is size-dependent. As reported recently by Lee et al., the quantum level spacing for particle sizes <5 nm can reach the energy of the LO phonon (~65 meV).[24] In Figure 5, we provide a qualitative model based on our experimental data. In smaller nanocrystals, the band-like levels that arise due to strong quantum confinement can host a continuum of photoexcited electrons. As the level spacing Δ approaches the LO phonon energy, coupling of LO phonons to the continuum gives rise to the observed strong Fano-line shapes in smaller nanocrystals. In larger nanocrystals, however, the level spacing is smaller than the LO phonon energy, concomitant with less quantum confinement. As a result, the interaction of the LO phonon with electrons is limited. This leads to a nearly symmetric Lorentzian line-shape. This tentative and qualitative physical picture is consistent with the recent DFT calculations of electronic structure of strongly confined Si QDs.[23] It is worth recalling that in hole-doped bulk Si the continuum is provided by intervalence band electronic excitations that overlap with the LO phonon energy.[19]

The second scenario is that the LO phonon interferes with a continuum of phototrapped electrons at the NC surface. In colloidal NCs, the chemically active NC surface can often become charged following photoexcitation,[25,26] and the lifetime of the trapped charges can vary from nanoseconds to seconds.[27] If trapping is prevalent in the course of CW excitation, a persistent NC charge may develop, and LO phonons are known to effectively couple to such charge density fluctuations.[28] Furthermore, in smaller NCs the rate and magnitude of the phototrapping may be enhanced owing to their greater surface-to-volume ratio. In such a scenario, smaller NCs could potentially exhibit more Fano coupling as seen in Figure 2. Phototrapping in our Si NCs is supported by temperature-dependent PL experiments (Figure S6 SI) which show clear signatures of emission quenching due to the presence of trap states at higher temperatures. The prevalence (and potentially high density) of surface traps on smaller NCs is further supported by recent studies demonstrating a reduction in photoluminescence quantum yield for smaller size NCs,[11] which may arise from the increased amorphous character at the NC surface. Such trapped charges were also found to enhance the Auger recombination rate, particularly with decreasing NC size.[29] The enhancement of trap state density with decreasing size has been observed in a number of prior studies,[30] including in Si NCs.[31]

However, we consider this explanation as the source of the electronic continuum to be improbable, as photocharging is a commonly observed phenomenon in other NC systems such as CdSe, where Fano-type optical phonon line shapes have not been reported.[1,32] Further, in CdSe NCs it has been shown that the trapped charges contribute significantly to e−ph coupling strength in spite of the lack of evidence of Fano interference. It is worth noting that in CdSe QDs the mechanism of e−ph coupling for LO phonons is via Fröhlich interaction, while in Si it is due to deformation potential.[33,34]

Finally, we also consider the possible presence of phonon−phonon Fano interference. In principle Fano interference merely requires interference of a discrete state with a continuum. The continuum may also arise due to phonons. Any change in phonon occupation numbers can be typically observed in a temperature-dependent experiment. However, we do not observe any noticeable temperature dependence of the LO phonon mode, reducing the likelihood of phonon−phonon interference as the source of Fano line shape (Figure S7). Thus, the more likely case is that the source of the electronic continuum is due to size-dependent quasi band-like states, as summarized in Figure 5.

The behavior of the LO mode in Si NCs we measured is in contrast to what has been observed for the LO mode in Si nanowires. In Si nanowires, as the excitation intensity is increased the line shape of the LO mode evolves from pure Lorentzian to Fano along with a systematic increase in its line width.[6] This was interpreted as arising from the coupling of the LO mode to the photoexcited carriers in the conduction band, as the incident laser energy was resonant with the interband transition. In the present case of Si NCs we observe a Fano line shape even at very low excitation intensities, corresponding to a local temperature of ~190 °C, which is much lower than the local temperature of Si nanowires in the prior study, estimated from the ratio of Stokes to anti-Stokes Raman intensities (see SI).

In conclusion, we have performed size-dependent, excitation intensity-dependent and excitation wavelength-dependent Raman scattering studies of colloidal Si NCs. The results suggest the interaction of the one-phonon LO mode in silicon with a continuum of electronic states. The dependence of line width upon excitation wavelength, and the progressive enhancement of the asymmetry with decreasing excitation wavelength cannot be described by the existing generalized

DOI: 10.1021/nl503671n
Nano Lett. 2015, 15, 1511−1516

theory developed for bulk silicon. The strong variation of line width, asymmetry, and frequency of the LO mode suggests that the density of states for the interfering electronic background varies sharply. These results suggest that the source of the electronic continuum is due to the size-dependent narrow band-like states that become populated by photoexcitation of carriers. Our observations are important for understanding and thereby controlling the mechanism of electron-LO phonon interaction, and carrier energy relaxation via LO phonon emission in Si nanocrystals. The results call for further theoretical investigations involving consideration of quantum level spacing, phonon-confinement, surface effects, electron–phonon coupling and the effect of band structure.

■ ASSOCIATED CONTENT

Supporting Information

Description of sample preparation, supporting figures, and details of background subtraction of raw data and description. This material is available free of charge via the Internet at http://pubs.acs.org.

■ AUTHOR INFORMATION

Corresponding Authors

*E-mail: matt.beard@nrel.gov.
*E-mail: manjunatha.dodderi@nrel.gov.

Notes

The authors declare no competing financial interest.

■ ACKNOWLEDGMENTS

We are thankful for helpful discussions with Dimitry Reznik. Work at NREL was supported by the U.S. Department of Energy Office of Science, Office of Basic Energy Sciences Solar Photochemistry program within the division of Chemical Sciences, Geosciences, and Biosciences under contract number DE-AC36-08GO28308. M.R. and J.A. acknowledge support from the National Science Foundation (NSF grant no. CHE1306398).

■ REFERENCES

(1) Sagar, D. M.; Cooney, R. R.; Sewall, S. L.; Dias, E. A.; Barsan, M. M.; Butler, I. S.; Kambhampati, P. *Phys. Rev. B* **2008**, *77*, 235321–235335.
(2) Norris, D. J.; Bawendi, M. G. *Phys. Rev. B* **1996**, *53*, 16338–16346.
(3) Klimov, V. I.; Mikhailovsky, A. A.; Xu, S.; Malko, A.; Hollingsworth, J. A.; Leatherdale, C. A.; Eisler, H.-J.; Bawendi, M. G. *Science* **2000**, *290*, 314–317.
(4) Richter, H.; Wang, Z. P.; Ley, L. *Solid State Commun.* **1981**, *39*, 625–629.
(5) Faraci, G.; Gibilisco, S.; Russo, P.; Pennisi, A. *Phys. Rev. B* **2006**, *73*, 33307.
(6) Gupta, R.; Xiong, Q.; Adu, C. K.; Kim, U. J.; Eklund, P. C. *Nano Lett.* **2003**, *3*, 627–631.
(7) Kumar, R.; Mavi, H. S.; Shukla, A. K.; Vankar, V. D. *J. Appl. Phys.* **2007**, *101*, 064315–064315–6.
(8) Fano, U. E. *Phys. Rev.* **1961**, *124*, 1866.
(9) Jurbergs, D.; Rogojina, E.; Mangolini, L.; Kortshagen, U. *Appl. Phys. Lett.* **2006**, *88*, 233116.
(10) Mangolini, L.; Thimsen, E.; Kortshagen, U. *Nano Lett.* **2005**, *5*, 655–659.
(11) Palomaki, P. K. B.; Blackburn, J. L.; Wheeler, L. M.; Johnson, J. C.; Neale, N. R. *Submitted*, 2015.
(12) Hessel, C. M.; Wei, J.; Reid, D.; Fujii, H.; Downer, M. C.; Korgel, B. A. *J. Phys. Chem. Lett.* **2012**, *3*, 1089–1093.
(13) Kendrick, C.; Klafehn, G.; Guan, T.; Anderson, I.; Shen, H.; Redwing, J.; Collins, R. *Sol. Energ. Mater. Sol. C* **2014**, *124*, 1–9.
(14) Mercaldo, L. V.; Esposito, E. M.; Veneri, P. D.; Fameli, G.; Mirabella, S.; Nicotra, G. *Appl. Phys. Lett.* **2010**, *97*, 153112.
(15) Rath, S.; Grigorescu, C.; Hsieh, M. L.; Voudouris, E.; Stradling, R. A. *Semiconductor Sci. Technol.* **2000**, *15*, L1.
(16) McEwen, G. D.; Wu, Y.; Zhou, A. *Biopolymers* **2010**, *93*, 171–177.
(17) Xia, H.; He, Y. L.; Wang, L. C.; Zhang, W.; Liu, X. N.; Zhang, X. K.; Feng, D.; Jackson, H. E. *J. Appl. Phys.* **1995**, *78*, 6705–6708.
(18) Sagar, D. M.; Fausti, D.; van Smaalen, S.; van Loosdrecht, P. H. M. *Phys. Rev. B* **2010**, *81*, 045124.
(19) Magidson, V.; Beserman, R. *Phys. Rev. B* **2002**, *66*, 195206.
(20) Contreras, G.; Sood, A. K.; Cardona, M.; Compaan, A. *Solid State Commun.* **1984**, *49*, 303–305.
(21) Cerdeira, F.; Fjeldly, T. A.; Cardona, M. *Phys. Rev. B* **1973**, *8*, 4734.
(22) Balkanski, M.; Jain, K. P.; Beserman, R.; Jouanne, M. *Phys. Rev. B* **1975**, *12*, 4328.
(23) Hapala, P.; Kůsová, K.; Pelant, I.; Jelínek, P. *Phys. Rev. B* **2013**, *87*, 195420.
(24) Lee, S.; Lee, Y.; Song, E. B.; Hiramoto, T. *Nano Lett.* **2013**, *14*, 71–77.
(25) Midgett, A. G.; Hillhouse, H. W.; Hughes, B. K.; Nozik, A. J.; Beard, M. C. *J. Phys. Chem. C* **2010**, *114*, 17486–17500.
(26) McGuire, J. A.; Sykora, M.; Robel, I.; Padilha, L. A.; Joo, J.; Pietryga, J. M.; Klimov, V. I. *ACS Nano* **2010**, *4*, 6087–6097.
(27) Beard, M. C. *J. Phys. Chem. Lett.* **2011**, *2*, 1282–1288.
(28) Giudici, P.; Goñi, A. R.; Thomsen, C.; Eberl, K.; Hauser, M. *Phys. Rev. B* **2006**, *73*, 45315.
(29) Cohn, A. W.; Schimpf, A. M.; Gunthardt, C. E.; Gamelin, D. R. *Nano Lett.* **2013**, *13*, 1810–1815.
(30) Uddin, A.; Wong, H. S.; Teo, C. C. *J. Nanosci. Nanotechnol.* **2012**, *12*, 7853–7859.
(31) Sychugov, I.; Juhasz, R.; Linnros, J. *Phys. Rev. B* **2005**, *71*, 115441.
(32) Baranov, A. V.; Rakovich, Y. P.; Donegan, J. F.; Perova, T. S.; Moore, R. A.; Talapan, D. V.; Rogach, A. L.; Masumoto, Y.; Nabiev, I. *Phys. Rev. B* **2003**, *68*, 165306.
(33) Kleinman, L. *Phys. Rev. B* **1962**, *128*, 2614–2621.
(34) Pötz, W.; Vogl, P. *Phys. Rev. B* **1981**, *24*, 2025–2037.

■ NOTE ADDED AFTER ASAP PUBLICATION

This paper was published on the Web on February 4, 2015. Additional text corrections were implemented throughout the paper, and the corrected version was reposted on February 5, 2015.

DOI: 10.1021/nl503671n
Nano Lett. 2015, 15, 1511–1516